Extracellular release of damaged mitochondria induced by cytotoxic conditioning exacerbates GVHD

Vijith Vijayan PhD[1] ∓, Hao Yan PhD[2]∓, Juliane K. Lohmeyer PhD[2], Kaylin A. Prentiss BS[3], Rachna V. Patil PhD[3], Giulia Barbarito PhD[3], Ivan Lopez BS[1], Aly Elezaby MD PhD[4], Kolten Peterson BS[3], Jeanette Baker PhD[2], Nicolai P. Ostberg MS[4], Alice Bertaina MD PhD[3], Robert S. Negrin MD[2], Daria Mochly-Rosen PhD[4], Kenneth Weinberg MD[3], Bereketeab Haileselassie MD MHS[1]

[1] Department of Pediatrics, Division of Critical Care Medicine, Stanford University School of Medicine, Stanford, CA, 94305; USA

[2] Department of Medicine, Division of Blood and Marrow Transplantation and Cellular Therapy, Stanford University School of Medicine, Stanford, CA, 94305; USA

[3] Department of Pediatrics, Division of Hematology, Oncology, Stem Cell Transplantation and Regenerative Medicine, Stanford University School of Medicine, Stanford, CA, 94305; USA

[4] Department of Chemical and Systems Biology, Stanford University School of Medicine, Stanford, CA, 94305; USA

∓ Shared first authorship

***Corresponding author:**

Bereketeab Haileselassie MD MHS

Department of Pediatrics, Division of Critical Care Medicine, Stanford University School of Medicine, Stanford, CA;

Email: bhailes3@stanford.edu

Telephone number: 650-497-7894

For original data, please contact bhailes3@stanford.edu

Abstract:

Despite therapeutic advancements, graft versus host disease (GVHD) is a major complication of hematopoietic stem cell transplantation (HSCT). Pathogen and damage associated molecular patterns released following pre-transplant conditioning play an important role in the initiation of GVHD. However, the role of extracellular mitochondria as an endogenous danger signal has not been fully explored. Herein, we report that cytotoxic conditioning with radiation leads to mitochondrial fission and dysfunction and impaired induction of PINK-1/PARKIN-dependent mitophagy, specifically in the intestinal mucosal layer. This radiation-induced imbalance in mitochondrial dynamics leads to the expulsion of mitochondria from intestinal epithelial cells in a cell-death independent manner both *in vitro* in cell culture supernatants of the Caco-2 cell line and *in vivo* in plasma of BALB/c mice. Extracellular mitochondria released upon irradiation were damaged, with functional impairment in ATP production and, increased protein carbonylation. Transplantation of isolated damaged mitochondria along with HSCT and splenocytes in a C57BL6/J → BALB/c mouse model of GVHD aggravated the disease-induced mortality. In mixed lymphocyte reactions, pre-incubation of BALB/c stimulator cells with syngeneic extracellular mitochondria increased the activation and proliferation of C57BL6/J responder T cells. In a cohort of pediatric patients who underwent HSCT, fractionated irradiation given with their conditioning regimen increased the abundance of circulating extracellular mitochondria and correlated with the incidence of GVHD. Our results suggest that modulation of extracellular mitochondria could be a novel therapeutic target to prevent GVHD after HSCT.

1. Background

Allogeneic hematopoietic stem cell transplantation (HSCT) is a therapeutic strategy to treat various oncologic, hematologic, immune and metabolic disorders by replacement of a patient's blood-forming stem cells by those of a healthy donor[1]. The broad application of allogeneic HSCT is limited by risk of complications, notably side effects of the pre-transplant conditioning needed to establish a hematopoietic graft and Graft-versus-host disease (GVHD), which is the leading cause of non-relapse mortality following HSCT[2]. GVHD occurs when alloreactive donor T lymphocytes recognize and direct an immune response against host cells[3,4]. Current prevention and treatment strategies for GVHD rely on immunosuppressive medications that largely target the T cells which mediate the disease[5]. However, therapies which target the upstream mechanisms involved in initiation of the GVHD immune response are limited.

Tissue damage from cytotoxic conditioning for HSCT significantly contributes to the onset of GVHD. One explanation for the interrelationship between tissue damage and GVHD is the local or systemic release of microbe- and tissue-derived byproducts (pathogen associated molecular patterns (PAMPs) and damage associated molecular patterns (DAMPs)), which prime host antigen presenting cells[6,7]. Recently, there has been a growing body of literature which implicates extracellular mitochondria as a link between tissue damage and inflammation in a variety of critical illnesses[8-12]. Because of their archaebacterial ancestry, mitochondria retain molecules, which are recognized by pattern recognition receptors of the innate and adaptive immune system[8,11,12]. Therefore, extracellular mitochondria, and associated byproducts, could play a significant role in the pathobiology of GVHD.

Extracellular release of mitochondrial content was previously thought to be a passive process secondary to cell death, but recent discoveries suggest that it can be an alternative mechanism for mitochondrial quality control, especially in settings where mitochondrial dynamics are impaired[13,14]. Our group as well as others have demonstrated that alterations in mitochondrial dynamics, in particular excessive mitochondrial fission, can mediate the extracellular release of damaged mitochondria following an inflammatory insult[15,16]. However, the impact of cytotoxic conditioning therapies on mitochondrial dynamics and the extracellular release of mitochondria have not been explored. In this article, we demonstrate that doses of irradiation relevant to HSCT conditioning significantly increased mitochondrial fission and release of damaged mitochondria in intestinal epithelial cells (IEC). Furthermore, using an *in vivo* model of HSCT, we show that extracellular mitochondria exacerbate incidence and mortality of GVHD. The pre-clinical findings are corroborated by an association between an increased extracellular mitochondrial content in circulation following conditioning and incidence of acute GVHD in a cohort of children undergoing HSCT.

2. Methods

Cell lines and *in vitro* treatment groups

The human colon epithelial cell-line, Caco-2, and human embryonic kidney (HEK293) (ATCC) were grown in DMEM containing 4mM L-glutamine, 4.5g/L glucose and 1mM sodium pyruvate (Corning), 10% FBS (Genesee Scientific) and 1% penicillin and streptomycin. Human umbilical vein endothelial cells (HUVECs) (ATCC) were grown in Endothelial Cell Medium (ECM) supplemented with endothelial cell GM (Promocell). All cells were maintained at 37°C

in an incubator with 5% CO2 and 100% humidity. All chemicals and reagents unless specified were purchased from Sigma Aldrich.

Analysis of mitochondrial morphology

Bowel tissue from BALB/c mice were carefully flushed using saline and fixed in 2.5% glutaraldehyde in 0.1 mol/l cacodylate buffer, pH-7.4. The fixed material was sectioned at the Stanford Electron Microscopy Facility per previous protocols [(16)] and tissue samples were evaluated using a JEOL 1230 transmission electron microscope. Imaging analysis was performed by a scientist blinded to treatment conditions (N.O.). Mitochondria were defined as altered based on previously validated criteria including: (i) decreased electron density of the matrix; (ii) fragmented and ballooned cristae; (iii) partial or complete separation of the outer and inner membranes [(17)].

Flow cytometric analysis of extracellular mitochondria

Extracellular mitochondria from cell culture supernatant were isolated by centrifugation (1500g for 5 min to remove cell debris, followed by 16000g for 20 min to isolate mitochondrial pellet). Platelet depleted plasma was centrifuged at 16000g for 20 min for isolating mitochondrial enriched pellet and was used for analysis of circulating cell-free mitochondria. Detection of mitochondria was performed by staining with MitoTracker™ Green FM (MTG) (Invitrogen) solution (100 nM for cell culture supernatant and 200 nM for plasma) or with an anti-TOM20 antibody. Mitochondrial membrane potential was analyzed by staining with Tetramethylrhodamine, Methyl Ester, Perchlorate (TMRM) (Invitrogen) (50 nM) with or without the addition of pyruvate/malate (5mM). Experiments were performed on NovoCyte Penteon

(Agilent technologies) or DXP10 (Cytek Biosciences) flow cytometers and analyzed using FlowJo™ (version 10) or Novocyte software.

Mitochondrial oxidative stress and cell death assay

Caco-2 cells were incubated with 5 µM MitoSOX™ (Invitrogen) in serum free growth medium for 20 min at 37°C per manufacture protocol. The median fluorescence intensity (MFI) of MitoSOX™ staining in cells was analyzed by flow cytometry as aforementioned. Cell death was quantified using media from experimental endpoints (in phenol red-free DMEM) to measure the percentage of released lactate dehydrogenase activity (LDH) using Cytotoxicity Detection Kit (Roche).

Mitochondrial ATP synthesis assay

ATP synthesis was determined using a luciferin/luciferase-based bioluminescence assay using 1 µg of mitochondria from each sample. The reaction mixture contained 15 µg D-luciferin, 0.15 µg firefly luciferase, 5mM pyruvate, 5mM malate, 0.5mM ADP and 15 µM DTT in a KCL-buffer (KCL (125mM), HEPES (10mM),), $MgCl_2$ (5mM) and K2HPO4 (2mM), pH 7.4). After addition of reaction mixture, the luminescence was recorded every 30 seconds for 40 minutes using a SpectraMax M2e microplate reader (Molecular Devices) and the concentration of ATP synthesized was determined using a standard curve plotted with known concentrations of ATP.

Bioenergetic profile

Caco-2 cells were plated at 30,000 cells per well on Seahorse XFe24 Cell Culture Microplate (Agilent). At the end of the experiment, cells were washed with Seahorse XF Media, supplemented with 1 mM pyruvate, 4 mM L-glutamine, and 10 mM D-glucose; per manufacturer

protocol. MitoStress assays were performed by treating the cells sequentially with 1 μM oligomycin, 1 μM carbonyl cyanide p-trifluoromethoxy phenylhydrazone (FCCP), and 0.5 μM rotenone/antimycin. Oxygen consumption rate (OCR) were measured after each compound using a Seahorse XFe24 Analyzer (Agilent).

Western blot analysis

Following isolation, all samples were resuspended in Laemmli buffer containing 2 mercaptoethanol, loaded on SDS–PAGE, and transferred on to 0.45 μm nitrocellulose membrane as described previously. Membranes were probed with the antibodies listed in Supplemental Table 1 and then visualized by enhanced chemiluminescence substrate (Biorad). Images acquired with Chemidoc Imager were analyzed with ImageJ to determine relative band intensity. For intracellular mitochondrial fractions or tissue lysates, equal amounts of protein from each sample were used. For detection of extracellular mitochondrial abundance from plasma and cell culture supernatant, equal volumes of the isolated fractions were used. Protein carbonylation was detected as described previously [(18)].

Allogeneic HSCT model

BALB/c mice (8-12 weeks) received fractionated total body irradiation [TBI] (2 doses of 4.4 Gy TBI) and were subsequently transplanted with $5x10^6$ T-cell depleted bone marrow cells alone or with $4x10^6$ splenocytes from C57BL6/J mice to induce GVHD [(19)]. Mitochondria enriched fraction from heart, liver and kidney was isolated in mannitol–sucrose (MS) buffer and treated with 1mM H_20_2 for 1 hr on ice and pelleted by centrifugation at 16000g for 20min. The mitochondrial pellet was resuspended in MS buffer and the protein concentration was estimated by Bradford's assay. 25 µg or 100 µg of mitochondria or MS vehicle were injected at the time of

transplantation along with the bone marrow cells in a total volume of 100 µL with or without donor splenocytes. Irradiated (8.8Gy) mice receiving either PBS, bone marrow, or bone marrow with mitochondria served as controls. Mice were monitored daily, and body weight and GVHD score were assessed twice weekly [20].

Mixed Lymphocyte Reaction

100,000 or 300,000 T-cell depleted splenocytes from BALB/C mice as stimulators were cocultured with 200,000 e-Fluor 670 (Invitrogen) stained responder T-cells isolated from splenocytes of GFP+ C57BL/6 mice in a 96 well plate at a stimulator to responder ratio of 0.5:1 and 1.5:1[21]. Where indicated, isolated heart mitochondria treated with H_20_2 from BALB/c mice were incubated with stimulator cells 24 hr prior to the addition of T-cells. Subsequently, the GFP+ responder T-cells were analyzed by flow cytometry for CD69 expression as an early activation marker and for proliferation based on the loss of e-Fluor 670 stain respectively. Staining with antibodies mentioned in Table 1 was performed as described previously. The gating strategy used for analysis excluded doublets, Zombie Yellow™ (Biolegend) stained dead cells and non-GFP expressing stimulator splenocytes.

Clinical cohort

Samples were obtained from a prospective cohort of children undergoing HSCT at Lucile Packard Children's Hospital (protocol ID: IRB 47220). Blood samples were processed to attain platelet depleted plasma per previous protocols [22]. 900 µL of MS buffer was added to 100 µL of plasma and centrifuged at 16000 g for 20 min. Supernatant was carefully removed and the mitochondrial pellet was resuspended in 100 µL of MS. Mitochondrial pellet was quantified by

MTG staining using flow cytometry as mentioned above.

Statistical analyses

Statistical analysis and graphing were performed using Prism 9.0 (Graphpad). Experimental results were evaluated based on the average of three or more independent experiments and calculated as mean values ± SD. Data distribution was evaluated with kernel density plots and the Shapiro-Wilk test for normality. For continuous variables, differences across groups were compared by one-way analysis of variance for normally distributed variables and Kruskal-Wallis test for nonparametric variables with Bonferroni correction for multiple comparisons. Cox proportional-hazards model was used to assess survival differences across groups. The nominal p value of <0.05 was used as statistically significant threshold.

2. Results:

Cytotoxic conditioning induces excessive mitochondrial fission and mitochondrial dysfunction in intestinal epithelial cells

To determine the effects of cytotoxic conditioning on mitochondrial dynamics and function, BALB/c mice were subjected to standard conditioning doses of irradiation (TBI-8.8 Gy). Subsequently, changes in mitochondrial architecture and function were evaluated in intestinal cells as target organ for GVHD. Electron microscopy of intestinal epithelial cells revealed mitochondrial damage with increased fission at 72 hrs, followed by a loss of cristae density as well as outer mitochondrial membrane (OMM) integrity at 120 hrs (Fig. 1A). Changes in mitochondrial morphology were quantified by a decrease in mitochondrial aspect-ratio (Control = 1.93±0.71 vs 8.8Gy = 0.81±0.8; p=0.001) and form factor (Control = 1.52±0.38 vs

8.8Gy = 0.507±0.34; p<0.001) (Supplemental Fig. S1A, S1B). Western blotting showed a 6-fold increase in mitochondrial translocation of dynamin related protein-1 (Drp1; p=0.0021), a key protein responsible for mitochondrial fission, in mitochondrial fractions from the small bowel of animals that received irradiation (Fig. 1B). Additionally, protein carbonylation assay of the mitochondrial fraction from small bowel showed a 1.8-fold increase in oxidative post-translational modifications (protein carbonylation; Control = 4.05±0.38 vs 8.8Gy = 7.6±2.49; p=0.05) following irradiation, suggesting an increase in oxidative stress (Fig. 1C).

To determine the impact of pre-HSCT irradiation conditioning on mitochondrial function, we treated intestinal epithelial cells (Caco-2) with similar doses of irradiation (5Gy and10Gy) and characterized changes in bioenergetics, mROS and ATP production. Irradiated Caco-2 cells exhibited a significant decrease in cellular respiration, represented by a drop in mitochondrial respiratory capacity (Basal OCR: p=0.008; ATP-linked OCR: p=0.002; maximal OCR: p=0.03) (Fig. 2A). These impairments in cellular respiration were associated with a dose-dependent increase in mitochondrial oxidative stress (MitoSox MFI fold change; 10Gy = 1.41±0.04; p=0.0006) and a decrease in complex I-dependent ATP production (fold change; 10Gy = 0.8 ± 0.09; p=0.005) (Fig. 2B, 2C).

Under physiologic conditions, mitochondrial damage leads to the induction of mitophagy, the cellular quality control response for selective removal of damaged mitochondria. Western blot analyses of bowel tissue revealed that both LC3-II levels (the lipidated form of LC3) and the polyubiquitination status of mitochondrial proteins were not changed following irradiation, indicating impaired induction in autophagy and mitophagy following irradiation (Supplemental Fig. S2A-S2E). Absence of Pink-1 stabilization and Parkin translocation in the mitochondrial fractions further corroborates the lack of mitophagy induction by pre-HSCT radiation

(Supplemental Fig. S2C). Analyses of intracellular mitochondrial content in total tissue lysates of small bowel showed no significant differences in the abundance of mitochondrial outer, inner membrane and matrix proteins or in the abundance of PGC1−α, the key transcriptional factor responsible for mitochondrial biogenesis, between control and irradiated mice (Supplemental Fig. S2A, S2B), suggesting that the lack of autophagy induction did not lead to accumulation of dysfunctional mitochondria within the cell.

Cytotoxic conditioning induces extracellular release of damaged mitochondria

Besides mitophagy, extracellular release of mitochondria has been proposed to be an alternate mechanism of mitochondrial quality control following cellular stress. Hence, we postulated that pre-HSCT conditioning would lead to the extracellular release of damaged mitochondria. To test this hypothesis, we examined both mitochondrial release into supernatants from cultured IEC and in plasma from mice treated with pre-HSCT irradiation. For the *in vitro* analyses, equal volumes of the cell culture supernatants from control and irradiated cells were subjected to differential centrifugation and the pellet was analyzed for mitochondrial presence by flow cytometry. Multiple mitochondrial markers including Mitotracker™ Green FM, mitochondrial membrane potential dye TMRM, and mitochondrial outer membrane protein (TOM20) were used to confirm that the yield from the differential centrifugation was indeed mitochondria (Supplemental Fig. S3A). Comparison of supernatants from control and irradiated Caco-2 cells revealed that irradiation caused approximately 50% increase in the extracellular release of mitochondria (Mitotracker + events fold change; 10Gy = 1.45±0.22; p=0.0002) (Fig. 3A). Similarly, western blot analyses using antibodies against the complexes of the electron transport chain (ETC) indicated increased levels of mitochondrial proteins in the extracellular milieu of

irradiated cells (Supplemental Fig. S3B). The increased release of mitochondria was independent of cell death, as measured by lack of significant difference in LDH release (Fig. 3B), suggesting that the expulsion of damaged mitochondria following irradiation was mediated by viable cells.

Comparison of extracellular mitochondria (ECM) function with that of isolated intracellular mitochondria (ICM) revealed that ECM have a significantly lower complex-I dependent ATP production (ATP (uM) per 1ug isolated mitochondria; ICM = 19.31± 3.74 uM vs ECM = 6.34 ± 3.5 uM, p=0.0006) (Supplemental Fig. S3C). Interestingly, the mitochondria released after irradiation demonstrated further impairment in ATP production (ATP (uM) per 1ug isolated mitochondria; Control = 6.34 ± 3.5 uM vs 10Gy = 4.4± 3 uM, p=0.026) as well as oxidative stress (DNP/SHDP fold change; 10Gy = 2.1± 0.3 uM, p=0.0003) (Fig. 3C, Supplemental Figs. S3D, S3E).

To determine the impact of cytotoxic conditioning on extracellular mitochondrial content *in vivo*, platelet-depleted plasma from control and irradiated BALB/c mice was collected. Flow cytometry of plasma with Mitrotracker Green stain revealed a significant increase in circulating cell-free mitochondria 24 hrs following irradiation (Mitotracker + events/60ul plasma; Control = 6,321±4,543 vs 8.8Gy = 58,793±27,567; p=0.0003), which persisted up to day 5 of analysis following conditioning (Fig. 3D, Supplemental Fig. S4A). The increase in cell-free mitochondria in plasma after irradiation was confirmed by western blot analysis of various mitochondrial proteins such as cytochrome c, HSP60 and ATP5A1 (Supplemental Fig. S4B). Next, we evaluated the function of the extracellular mitochondria by testing their ability to hyperpolarize the mitochondrial membrane potential in response to complex-I substrates (pyruvate and malate (P+M)). Addition of complex-I substrates to cell-free mitochondria isolated from plasma of non-irradiated mice significantly induced the resting membrane potential, quantified by fluorescence

intensity of TMRM. However, mitochondria from plasma of irradiated mice exhibited diminished hyperpolarization (fold change; Control= 5.7±1.2 vs 8.8Gy = 2.6±0.87; $p<0.0001$) (Fig. 3E), indicating that extracellular mitochondria from irradiated mice have impairments in the production or maintenance of the proton motive force. This was further confirmed by evaluating complex-I dependent ATP production which demonstrated that mitochondria from plasma of irradiated mice produced less ATP than unirradiated controls (ATP (uM) per 1ug isolated mitochondria; Control = 2.6 ± 0.35 uM vs 8.8Gy = 0.35± 0.26 uM, $p=0.001$) (Fig. 3F and Supplemental Fig. S4C).

Extracellular mitochondria increase activation and proliferation of T-cells and aggravates the incidence and severity of GVHD in murine models

To test the hypothesis that extracellular mitochondria stimulate host APCs to increase the allogenic response of donor T-cells, we used an *in vitro* mixed lymphocyte reaction (MLR) with responder T-cells from C57BL/6J mice and stimulator T-cell depleted splenocytes from BALB/C mice. When using a sub-optimal stimulator to responder ratio (S/R 0.5:1), pre-incubation of stimulators with syngeneic damaged mitochondria increased the expression of the early activation marker CD69 on the allogeneic responder T-cells in a dose-dependent manner (Fig. 4A). The enhancing effect of mitochondria on the stimulation of the allogeneic T-cells was not observed when the S/R was increased to 1.5:1, consistent with maximal activation of responders s had been achieved at this ratio (Fig. 4A). In contrast, analysis of proliferation of allogeneic T-cells after day 5 of MLR indicated that extracellular mitochondria increased proliferation at both S/R of 0.5:1 and 1.5:1 (statistically significant at S/R 1.5:1), indicating that proliferation could

still be enhanced by pre-incubation of the stimulators with mitochondria, even though the S/R ratio was optimal for T-cell activation (Fig. 4B).

Next**,** to study the impact of extracellular mitochondria on incidence and severity of aGVHD, we utilized a well-characterized aGVHD model [19] in which T-cell depleted BM cells ($5x10^6$ cells/mouse) and splenocytes ($4x10^6$ cells/mouse) from C57BL6/J donors were transplanted into irradiated BALB/c recipient mice, which received graded doses of damaged mitochondria (0, 25, 100 ug). Results demonstrated that BALB/c mice that were transplanted with HSCs and splenocytes had a median survival of 31 days, which was worsened when co-treated with extracellular mitochondria, (median survival; BM + splenocyte + mitochondria (25ug) = 21days, p=0.0042; BM + splenocyte + mitochondria (100ug) = 14 days, p= 0.0014) (Figs. 5A, 5B).

To confirm that the accelerated mortality following treatment with damaged extracellular mitochondria is GVHD-specific, we transplanted irradiated BALB/c recipient mice with T cell-depleted BM cells ($5x10^6$ cells/mouse) alone from C57BL6/J donors with and without damaged mitochondria (100 ug), but without donor splenocytes. Results demonstrated no significant mortality difference between the two groups (Fig. 5A), consistent with the impact of damaged extracellular mitochondria being GVHD-specific.

Association of increased circulating mitochondria with conditioning and GVHD in children undergoing HSCT

To validate the clinical relevance of our *in vitro* and *in vivo* findings, we evaluated changes in extracellular mitochondrial content from platelet-depleted plasma samples of pediatric patients undergoing HSCT. Transplant indications for the cohort consisted of

hematologic cancers, nonhematologic cancers and bone marrow failure syndromes requiring diverse therapies prior to initiation of HSCT (Table 1). When stratified by incidence of GVHD, we did not observe any significant differences in patient demographics, indication for transplant, HLA molecular typing or GVHD prophylaxis (Table 1). We observed an overall increase in extracellular mitochondria following conditioning, which was most pronounced in the subset of patients who received TBI as a component of their conditioning regimen, (Mitotracker + events/60ul plasma fold change from baseline; day 0 = 4.2 ± 1.5 p= 0.047, day 7= 2.43± 0.71 p= 0.043, day 14= 3.7± 1.3 p= 0.016), (Fig. 6A). Compared to those who did not develop GVHD, the patients with GVHD had a 6-fold higher level of extracellular mitochondrial content on Day 0 (day of transplantation) (Mitotracker + events/60ul plasma; no-GVHD = 11,117±6,327 vs GVHD = 66,330±24,800, p=0.04), when compared to those who did not develop GVHD (Fig. 6B).

Discussion

GVHD is the most common complication of HSCT, and the leading cause of non-relapse mortality following transplant[(1)]. Current GVHD prophylaxis strategies consist primarily of globally immune suppressive drugs that largely target T cells [(5)]. Although allogeneic T cells have been long understood to be a prerequisite for GVHD, the initiation of GVHD also depends on tissue damage, typically resulting from the cytotoxic therapies given as pre-transplant conditioning to ensure HSC engraftment [(1-4)]. Conditioning-induced damage to mucosa, including the intestine, allows translocation of bacteria which express PAMPs while simultaneously leading to the release of endogenously derived DAMPs [(6,,7)]. Whereas previous studies have linked GVHD severity with the release of these danger signals, the role of

extracellular mitochondria in the pathogenesis of GVHD has not been adequately studied. Extracellular mitochondria could constitute a novel danger signal in GVHD pathogenesis in that they are endogenous, but, because of their archaebacterial origin, express molecules typical of PAMPs.

Here we demonstrate that doses of radiation similar to those used as pre-HSCT conditioning cause mitochondrial dysfunction and alteration in mitochondrial dynamics, resulting in extracellular mitochondrial release both *in vitro* (Figs. 2, 3A-C) and *in vivo* (Figs. 1, 3D-F). The presence of circulating extracellular mitochondria exacerbates GVHD-associated mortality (Fig. 5). The clinical relevance of these observations is highlighted by the demonstration that TBI-based conditioning increased the level of circulating cell-free mitochondria in patients undergoing HSCT and correlated with the incidence of acute GVHD post-transplant (Fig. 6).

Mitochondrial dynamics and extracellular release

Mitochondrial dynamics, the balance between mitochondrial fusion, fission, biogenesis and mitophagy, plays an essential role in mitochondrial quality control [(23)]. Once damaged, mitochondria are segregated from the network by Drp1-dependent mitochondrial fission and subsequently, removed by mitochondrial autophagy[(24)]. While irradiation significantly increased mitochondrial damage (Fig. 1A), we did not observe changes in either key regulators of mitophagy (Supplemental Figs. S2A, S2C-F) or accumulation of intracellular mitochondria following conditioning (Supplemental Figs. S2A, S2B). Together, this suggests that fragmented mitochondria are cleared by an alternate mechanism after irradiation. Recent publications have suggested that extracellular release of damaged mitochondria is an alternate mechanism by

which cells maintain quality control, especially when canonical mechanisms of mitochondrial dynamics are impaired [13,25]. Our data demonstrating an increase in damaged extracellular mitochondria following TBI (Figs. 3A, 3D), independent of cell death (Fig. 3B), suggest that this mechanism plays an important role in the clearance of mitochondria following conditioning.

The underlying mechanism for the extracellular release of mitochondria has been a topic of intense investigation in recent years. Although the consensus is that cell-free mitochondria are a byproduct of intracellular mitochondrial quality control, various mechanisms leading to their generation and release have been proposed. Tan et al, described a phenomenon termed 'secretory autophagy' that mediates the release of mitochondria in the absence of mATG8-conjugation machinery *in vitro*[25]. Independently, Bao et al, reported mitochondrial expulsion in the form of 'mitolysosome exocytosis' in flunarizine-treated neuronal progenitor cells[26]. Work from our group has shown that excessive mitochondrial fission is associated with the release of dysfunctional mitochondria to the extracellular milieu in pre-clinical models of sepsis and neuroinflammation[15,16]. Therefore, we propose that radiation induces mitochondrial fission and impairs mitochondrial autophagy, thereby contributing to the release of extracellular mitochondria observed in this study. Supporting this notion, a recent study reported that baicalin, a flavonoid purified from the plant *Scutellaria baicalensis*, induced autophagy and preserved mitochondrial architecture in the intestinal epithelium and reduced intestinal aGVHD[27]. However, the extracellular release of mitochondria was not explored in the aforementioned study and thus future studies are necessary to determine if extracellular release of mitochondria can be modulated by inducing mitophagy and blocking excessive mitochondrial fission.

Immunomodulatory role of extracellular mitochondria

Mitochondria contain byproducts that can induce immune cell activation via multiple mechanisms, including, mtDNA-mediated TLR9 signaling, N-formyl peptide-mediated receptor activation, cardiolipin-mediated pro-inflammatory activation and ATP-mediated signaling through purinergic receptors [11,28,29]. Specific to GVHD, Koehn et.al. demonstrated that extracellular ATP exacerbates GVHD-associated mortality in pre-clinical models by impairing the anti-inflammatory effect of donor myeloid-derived suppressor cells (MDSC)[30]. Our results demonstrate that release of mitochondria to the extracellular space can also stimulate host APCs and promote the activation of donor T cells (Figs. 4A-B). Much of our current knowledge on the immune stimulation by mitochondria comes from studying specific mitochondrial byproducts (mtDAMPs) in isolation. With the recent discoveries that intact cell-free mitochondria can be found in circulation[31,32], a comprehensive characterization of the many potential immunostimulatory molecules is required to understand the impact of extracellular mitochondria on the immune response under physiologic and pathologic conditions.

Of note, cell-free mitochondria are found in the plasma of healthy volunteers[32]. However, the functional competency of these mitochondria is debated[31,32]. In this study, we report the presence of outer membrane, ETC and matrix proteins in the extracellular mitochondrial isolates, suggesting the presence of intact mitochondria. Furthermore, when provided with the substrate for complex I, these extracellular mitochondria hyperpolarized their membrane potential and produced ATP, albeit with a reduced capacity in comparison to isolated intracellular mitochondria (Supplemental Fig. S3C). Interestingly, these functions were further diminished in mitochondria present post-conditioning, suggesting that in addition to the abundance, the functional properties or degree of damage of extracellular mitochondria might be a determining factor that influences the pathogenesis of GVHD.

Albeit our results are focused on mitochondrial damage in intestinal epithelial cells, it is highly likely that other cell types in various end-organs are sensitive to conditioning mediated mitochondrial damage and therefore contribute to the extracellular mitochondrial content in the circulation. This is supported by our observations of impaired bioenergetics and oxidative stress in both HEK cells and HUVECs following irradiation (Fig. S5).

While the present studies introduce a new pathogenic mechanism for GVHD and suggests potential novel approaches to GVHD prevention, several questions need to be addressed in future investigations. Our results have shown that extracellular mitochondria increase incidence and severity of acute GVHD. However, the cell populations which respond to the extracellular mitochondria and initiate the cellular signaling necessary for donor T cell activation requires further investigation. Additionally, our clinical observations need to be validated in a larger cohort of patients and be able to segregate multiple conditioning methods and its impact on extracellular mitochondrial levels and GVHD.

Current GVHD prophylaxis strategies consist of globally immune suppressive drugs that are prone to complications including opportunistic infections, viral reactivation as well as engraftment failure. Future studies aiming to block the release of mitochondria into the extracellular milieu or scavenge existing extracellular mitochondria from circulation as a prophylaxis before HSCT are warranted to determine whether extracellular mitochondria could serve as a clinically useful target for prevention of GVHD, possibly without risk of immune suppression

Author Contribution: V.V, H.Y, K.W and B.H. contributed to manuscript preparation. V.V, K.W and B. H generated the hypothesis. R.S.N, A.B and D.M-R aided with experimental design. V.V, H.Y, B.H, J.K.L, K.A.P, A.E, K.P, J.B, conducted the *in vitro* and animal experiments and analysis. V.V, R.V.P, G.B, I.L collected and conducted the analysis on the clinical samples. N.O preformed the blinded imaging analysis. All the authors reviewed and edited the manuscript.

Conflict of Interest: None of the authors have any relevant conflict of interest to declare

Reference:

1. Blazar BR, Murphy WJ, Abedi M. Advances in graft-versus-host disease biology and therapy. Nat Rev Immunol. 2012 May 11;12(6):443-58. doi: 10.1038/nri3212. PMID: 22576252; PMCID: PMC3552454.
2. Wu SR, Reddy P. Tissue tolerance: a distinct concept to control acute GVHD severity. Blood. 2017 Mar 30;129(13):1747-1752. doi: 10.1182/blood-2016-09-740431. Epub 2017 Feb 2. PMID: 28153825; PMCID: PMC5374290.
3. Magenau J, Runaas L, Reddy P. Advances in understanding the pathogenesis of graft-versus-host disease. Br J Haematol. 2016 Apr;173(2):190-205. doi: 10.1111/bjh.13959. Epub 2016 Mar 27. PMID: 27019012.
4. Zeiser R. Advances in understanding the pathogenesis of graft-versus-host disease. Br J Haematol. 2019 Dec;187(5):563-572. doi: 10.1111/bjh.16190. Epub 2019 Oct 6. PMID: 31588560.
5. Gooptu M, Antin JH. GVHD Prophylaxis 2020. Front Immunol. 2021 Apr 7;12:605726. doi: 10.3389/fimmu.2021.605726. PMID: 33897681; PMCID: PMC8059368.
6. Ramadan A, Paczesny S. Various forms of tissue damage and danger signals following hematopoietic stem-cell transplantation. Front Immunol. 2015 Jan 28;6:14. doi: 10.3389/fimmu.2015.00014. PMID: 25674088; PMCID: PMC4309199.
7. Toubai T, Mathewson ND, Magenau J, Reddy P. Danger Signals and Graft-versus-host Disease: Current Understanding and Future Perspectives. Front Immunol. 2016 Nov 29;7:539. doi: 10.3389/fimmu.2016.00539. PMID: 27965667; PMCID: PMC5126092.
8. Nakahira K, Hisata S, Choi AM. The Roles of Mitochondrial Damage-Associated Molecular Patterns in Diseases. Antioxid Redox Signal. 2015 Dec 10;23(17):1329-50. doi: 10.1089/ars.2015.6407. Epub 2015 Aug 17. PMID: 26067258; PMCID: PMC4685486.
9. Grazioli S, Pugin J. Mitochondrial Damage-Associated Molecular Patterns: From Inflammatory Signaling to Human Diseases. Front Immunol. 2018 May 4;9:832. doi: 10.3389/fimmu.2018.00832. PMID: 29780380; PMCID: PMC5946030.
10. Weiss SL, Zhang D, Bush J, Graham K, Starr J, Tuluc F, Henrickson S, Kilbaugh T, Deutschman CS, Murdock D, McGowan FX Jr, Becker L, Wallace DC. Persistent Mitochondrial Dysfunction Linked to Prolonged Organ Dysfunction in Pediatric Sepsis. Crit Care Med. 2019 Oct;47(10):1433-1441. doi:10.1097/CCM.0000000000003931. PMID: 31385882; PMCID: PMC7341116.
11. Miliotis S, Nicolalde B, Ortega M, Yepez J, Caicedo A. Forms of extracellular mitochondria and their impact in health. Mitochondrion. 2019 Sep;48:16-30. doi: 10.1016/j.mito.2019.02.002. Epub 2019 Feb 14. PMID: 30771504
12. Krychtiuk KA, Ruhittel S, Hohensinner PJ, Koller L, Kaun C, Lenz M, Bauer B, Wutzlhofer L, Draxler DF, Maurer G, Huber K, Wojta J, Heinz G, Niessner A, Speidl WS. Mitochondrial DNA and Toll-Like Receptor-9 Are Associated With Mortality in Critically Ill Patients. Crit Care Med. 2015 Dec;43(12):2633-41. doi: 10.1097/CCM.0000000000001311. PMID: 26448617.
13. Choong CJ, Okuno T, Ikenaka K, Baba K, Hayakawa H, Koike M, Yokota M, Doi J, Kakuda K, Takeuchi T, Kuma A, Nakamura S, Nagai Y, Nagano S, Yoshimori T, Mochizuki H. Alternative mitochondrial quality control mediated by extracellular release. Autophagy. 2021 Oct;17(10):2962-2974. doi: 10.1080/15548627.2020.1848130. Epub 2020 Dec 10. PMID: 33218272; PMCID: PMC8525996.

14. Tan HWS, Lu G, Shen HM. Autophagic secretion of mitochondria (ASM): an alternative way for getting rid of damaged mitochondria. Autophagy. 2023 Feb;19(2):739-741. doi: 10.1080/15548627.2022.2107310. Epub 2022 Aug 8. PMID: 35900940; PMCID: PMC9851247.
15. Mukherjee R, Tompkins CA, Ostberg NP, Joshi AU, Massis LM, Vijayan V, Gera K, Monack D, Cornell TT, Hall MW, Mochly-Rosen D, Haileselassie B. Drp1/Fis1-Dependent Pathologic Fission and Associated Damaged Extracellular Mitochondria Contribute to Macrophage Dysfunction in Endotoxin Tolerance. Crit Care Med. 2022 Jun 1;50(6):e504-e515. doi: 10.1097/CCM.0000000000005437. Epub 2022 Jan 24. PMID: 35067534; PMCID: PMC9133053.
16. Joshi AU, Minhas PS, Liddelow SA, Haileselassie B, Andreasson KI, Dorn GW 2nd, Mochly-Rosen D. Fragmented mitochondria released from microglia trigger A1 astrocytic response and propagate inflammatory neurodegeneration. Nat Neurosci. 2019 Oct;22(10):1635-1648. doi: 10.1038/s41593-019-0486-0. Epub 2019 Sep 23. Erratum in: Nat Neurosci. 2021 Feb;24(2):289. PMID: 31551592; PMCID: PMC6764589.
17. Picard M, White K, Turnbull DM. Mitochondrial morphology, topology, and membrane interactions in skeletal muscle: a quantitative three-dimensional electron microscopy study. J Appl Physiol (1985). 2013 Jan 15;114(2):161-71. doi: 10.1152/japplphysiol.01096.2012. Epub 2012 Oct 25. PMID: 23104694; PMCID: PMC3544498.
18. Colombo G, Clerici M, Garavaglia ME, Giustarini D, Rossi R, Milzani A, Dalle-Donne I. A step-by-step protocol for assaying protein carbonylation in biological samples. J Chromatogr B Analyt Technol Biomed Life Sci. 2016 Apr 15;1019:178-90. doi: 10.1016/j.jchromb.2015.11.052. Epub 2015 Dec 2. PMID: 26706659.
19. Beilhack A, Schulz S, Baker J, Beilhack GF, Nishimura R, Baker EM, Landan G, Herman EI, Butcher EC, Contag CH, Negrin RS. Prevention of acute graft-versus-host disease by blocking T-cell entry to secondary lymphoid organs. Blood. 2008 Mar 1;111(5):2919-28. doi: 10.1182/blood-2007-09-112789. Epub 2007 Nov 7. PMID: 17989315; PMCID: PMC2254542.
20. Cooke KR, Kobzik L, Martin TR, Brewer J, Delmonte J Jr, Crawford JM, Ferrara JL. An experimental model of idiopathic pneumonia syndrome after bone marrow transplantation: I. The roles of minor H antigens and endotoxin. Blood. 1996 Oct 15;88(8):3230-9. PMID: 8963063.
21. Nishikii H, Kim BS, Yokoyama Y, Chen Y, Baker J, Pierini A, Alvarez M, Mavers M, Maas-Bauer K, Pan Y, Chiba S, Negrin RS. DR3 signaling modulates the function of Foxp3+ regulatory T cells and the severity of acute graft-versus-host disease. Blood. 2016 Dec 15;128(24):2846-2858. doi: 10.1182/blood-2016-06-723783. Epub 2016 Oct 19. PMID: 27760760; PMCID: PMC5159706.
22. Lacroix R, Judicone C, Mooberry M, Boucekine M, Key NS, Dignat-George F; The ISTH SSC Workshop. Standardization of pre-analytical variables in plasma microparticle determination: results of the International Society on Thrombosis and Haemostasis SSC Collaborative workshop. J Thromb Haemost. 2013 Apr 2:10.1111/jth.12207. doi: 10.1111/jth.12207. Epub ahead of print. Erratum in: J Thromb Haemost. 2017 Jun;15(6):1236. PMID: 23551930; PMCID: PMC4395506.
23. Picca A, Mankowski RT, Burman JL, Donisi L, Kim JS, Marzetti E, Leeuwenburgh C. Mitochondrial quality control mechanisms as molecular targets in cardiac ageing. Nat Rev

Cardiol. 2018 Sep;15(9):543-554. doi: 10.1038/s41569-018-0059-z. PMID: 30042431; PMCID: PMC6283278.

24. Kornfeld OS, Hwang S, Disatnik MH, Chen CH, Qvit N, Mochly-Rosen D. Mitochondrial reactive oxygen species at the heart of the matter: new therapeutic approaches for cardiovascular diseases. Circ Res. 2015 May 22;116(11):1783-99. doi: 10.1161/CIRCRESAHA.116.305432. PMID: 25999419; PMCID: PMC4443500.
25. Tan HWS, Lu G, Dong H, Cho YL, Natalia A, Wang L, Chan C, Kappei D, Taneja R, Ling SC, Shao H, Tsai SY, Ding WX, Shen HM. A degradative to secretory autophagy switch mediates mitochondria clearance in the absence of the mATG8-conjugation machinery. Nat Commun. 2022 Jun 28;13(1):3720. doi: 10.1038/s41467-022-31213-7. PMID: 35764633; PMCID: PMC9240011.
26. Bao F, Zhou L, Zhou R, Huang Q, Chen J, Zeng S, Wu Y, Yang L, Qian S, Wang M, He X, Liang S, Qi J, Xiang G, Long Q, Guo J, Ying Z, Zhou Y, Zhao Q, Zhang J, Zhang D, Sun W, Gao M, Wu H, Zhao Y, Nie J, Li M, Chen Q, Chen J, Zhang X, Pan G, Zhang H, Li M, Tian M, Liu X. Mitolysosome exocytosis, a mitophagy-independent mitochondrial quality control in flunarizine-induced parkinsonism-like symptoms. Sci Adv. 2022 Apr 15;8(15):eabk2376. doi: 10.1126/sciadv.abk2376. Epub 2022 Apr 13. PMID: 35417232; PMCID: PMC9007515.
27. Sun X, Pisano M, Xu L, Sun F, Xu J, Zheng W, Liu X, Zhang Y, Sun R, Cui X. Baicalin regulates autophagy to interfere with small intestinal acute graft-versus-host disease. Sci Rep. 2022 Apr 21;12(1):6551. doi: 10.1038/s41598-022-10564-7. PMID: 35449393; PMCID: PMC9023573.
28. Todkar K, Chikhi L, Desjardins V, El-Mortada F, Pépin G, Germain M. Selective packaging of mitochondrial proteins into extracellular vesicles prevents the release of mitochondrial DAMPs. Nat Commun. 2021 Mar 30;12(1):1971. doi: 10.1038/s41467-021-21984-w. PMID: 33785738; PMCID: PMC8009912.
29. Koenig A, Buskiewicz-Koenig IA. Redox Activation of Mitochondrial DAMPs and the Metabolic Consequences for Development of Autoimmunity. Antioxid Redox Signal. 2022 Mar;36(7-9):441-461. doi: 10.1089/ars.2021.0073. PMID: 35352943; PMCID: PMC8982130.
30. Koehn BH, Saha A, McDonald-Hyman C, Loschi M, Thangavelu G, Ma L, Zaiken M, Dysthe J, Krepps W, Panthera J, Hippen K, Jameson SC, Miller JS, Cooper MA, Farady CJ, Iwawaki T, Ting JP, Serody JS, Murphy WJ, Hill GR, Murray PJ, Bronte V, Munn DH, Zeiser R, Blazar BR. Danger-associated extracellular ATP counters MDSC therapeutic efficacy in acute GVHD. Blood. 2019 Nov 7;134(19):1670-1682. doi: 10.1182/blood.2019001950. PMID: 31533918; PMCID: PMC6871306.
31. Al Amir Dache Z, Otandault A, Tanos R, Pastor B, Meddeb R, Sanchez C, Arena G, Lasorsa L, Bennett A, Grange T, El Messaoudi S, Mazard T, Prevostel C, Thierry AR. Blood contains circulating cell-free respiratory competent mitochondria. FASEB J. 2020 Mar;34(3):3616-3630. doi: 10.1096/fj.201901917RR. Epub 2020 Jan 19. PMID: 31957088.
32. Stier A. Human blood contains circulating cell-free mitochondria, but are they really functional? Am J Physiol Endocrinol Metab. 2021 May 1;320(5):E859-E863. doi: 10.1152/ajpendo.00054.2021. Epub 2021 Mar 15. PMID: 33719587.

Table 1:

	TOTAL	GVHD	No-GVHD	p
N	17	9	8	
Age at transplant				
Median (q25-q75)	11 (7.5-14.5)	11(6.5-14.5)	13 (8.7-16.25)	0.41
Sex (M, %)	8 (47.1)	4 (44)	4(50)	0.97
Primary diagnosis				
ALL (%)	6 (35)	5 (55.6)	1 (12.5)	0.19
AML (%)	5 (29.5)	2 (22.2)	3 (37.5)	0.45
MDS (%)	2 (11.7)	1 (11.1)	1(12.5)	0.99
Severe Aplastic Anemia (%)	2 (11.7)	0 (0)	2 (25)	0.17
Other (%)	2 (11.7)	1 (11.1)	1 (12.5)	0.93
HLA molecular typing				
Matched related	3 (17.6)	3 (33.3)	0 (0)	0.16
Matched unrelated	0 (0)	0 (0)	0 (0)	NA
Mismatched related	9 (53)	4 (44.4)	5(62.5)	0.89
Mismatched unrelated	5 (29.4)	2 (22.2)	3 (37.5)	0.76
Patient CMV serostatus				
Positive (%)	2 (11.7)	2 (22.2)	0 (0)	0.39
GVHD prophylaxis				
alpha beta T-cell depletion	8 (47.1)	4 (44.4)	4 (50)	0.97
Tacro, MTX	3 (17.6)	3 (33.3)	0	0.21
Tacro, MMF	5 (29.4)	2 (22.2)	3 (37.5)	0.22
CsA, Tacro, MMF	1 (5.9)	0	1 (12.5)	0.58
Conditioning regimen				
Low dose TBI (≤4Gy)	7	3 (33.3)	4 (50)	0.8
High dose TBI (≥10Gy)	10	6 (66.6)	4 (50)	0.78
rATG	12	6 (66.6)	6 (75)	0.93
Thiotepa / Fludarabine	9	5 (55.6)	4 (50)	0.58
Melphalan / Clofarabine	2	2 (22.2)	0	NA
Busulfan	1	1 (11.1)	0	NA
Fludarabine / Cyclophosphamide	3	0	3 (37.5)	NA
Melphalan/ Thiotepa / Clofarabine	1	0	1 (12.5)	NA

Figure legend:

1) **TBI induces mitochondrial fission and mitochondrial protein carbonylation in the small intestine**

   (A) Small bowel of BALB/c mice treated with TBI was resected at the indicated time points and evaluated for changes in mitochondrial architecture. Representative electron micrograph for each time point is shown. Enriched mitochondrial fractions isolated 24 h post TBI from small bowel of mice (B) A representative Western blot probed with antibodies against DRP1 for mitochondrial fission, and VDAC-1 for total mitochondrial content (left) and densitometric protein quantification (n=3) (right) is shown. (C) A representative Western blot derivatized with dinitrophenylhydrazine and probed with antibodies against DNP for protein carbonylation and VDAC-1 for total mitochondrial content (left) and densitometric protein quantification (n =3) (right) is shown . CT: control non irradiated mice. (*$p < 0.05$, **$p < 0.01$. n - number of mice).

2) **Irradiation leads to mitochondrial dysfunction in hCaco-2 cells**

   Caco-2 cells were irradiated at the indicated doses, cultured for an additional 24 hrs and subjected to various mitochondrial functional assays (A) A representative Seahorse plot of the Mito Stress assay and bar graphs of the respiratory parameters calculated from the test and normalized to the total protein content ($n \geq 3$). (B) The median fluorescence intensity of cells stained with MitoSOX^{TM} and analyzed by flow cytometry is shown as relative fold inductions in relation to control non-irradiated cells (CT) (n=3). Cells treated with 5 µM antimycin-A for 3 h served as a positive control for the assay. (C) ATP

production in 1ug of isolated mitochondria from non-irradiated (CT) and irradiated (10Gy) Caco-2 cells when provided with pyruvate and malate as substrates. A representative plot of luciferase activity recorded over time (left) and the relative concentration of ATP calculated are shown (n=4). (*$p < 0.05$, **$p < 0.01$, ***$p < 0.001$, ****$p < 0.0001$; n- number of independent experiments).

3) Irradiation leads to release of damaged extracellular mitochondria

Extracellular mitochondria isolated from cell-culture supernatants of non-irradiated (CT) and irradiated (10Gy) Caco-2 cells was subjected to (A) MTG staining and analyzed by flow cytometry. The relative MTG positive events are shown as fold induction (n=7). (B) Cell culture supernatants from non-irradiated (CT) and irradiated (10Gy) Caco-2 cells cultured for 24 h were subjected to LDH assay and the results are represented as % cytotoxicity. Staurosporine (1 µM) treatment for 12 hrs was used as a positive control for the experiment (n=3). (C) complex-I dependent ATP-production. A representative plot of luciferase activity recorded over time is shown. (D) Extracellular mitochondrial content in plasma of BALB/c mice 24 hrs following TBI (8.8Gy) was stained with MTG was analyzed by flow cytometry. The number of MTG positive events detected in 60 µL of plasma is shown; CT- non-irradiated control mice (n=7). (E) Extracellular mitochondria isolated from the plasma of BALB/C mice after 24 hrs following TBI (8.8 Gy) was subjected to TMRM staining in the presence or absence of complex-I substrates (pyruvate and malate) and analyzed by flow cytometry. The median fluorescence intensity of TMRM calculated is represented as relative fold induction (n=4). (F) Mitochondria isolated from the plasma of BALB/C mice 24 hrs following TBI (8.8Gy) or non-

irradiated (CT) was subjected to complex-I-dependent ATP production (n=3). (*$p < 0.05$, **$p < 0.01$, ***$p < 0.001$, ****$p < 0.0001$; n- number of independent experiments).

4) Extracellular mitochondria increase allogeneic T-cell activation and proliferation *in vitro*

In vitro MLR between C57BL/6J responder T-cells and BALB/c T-cell depleted splenocytes was set up as described in the Methods section. (A) Cells were stained with a CD69 antibody and representative dot plots for the expression of CD69 on GFP-expressing responder T-cells after 48 hrs of MLR (S/R: 0.5 to 1) with the indicated doses of mitochondria (Mito) (left) and the mean percentage CD69 positive T-cells in both S/R ratios (right) are shown. (B) Representative histograms after 120 hrs of MLR with the indicated treatments showing the percentage of proliferat responder T-cells in S/R: 1.5 to 1 (left) and relative proliferation index (RPI) for both S/R ratios was calculated using the equation: RPI = (stimulated T-cells with or without mitochondrial treatment - non stimulated T-cells)/ stimulated T-cells without mitochondrial treatment (right) are shown (n=3). (*$p < 0.05$, **$p < 0.01$, ***$p < 0.001$; n- number of independent experiments).

5) Extracellular mitochondria aggravate GVHD-induced mortality

Hematopoietic stem cells (HSC) from bone marrow ($5x10^6$ cells) and splenocyte ($4x10^6$ cells) from C57BL6/J mice were transplanted into BALB/c mice following TBI conditioning to model acute GVHD. At the time of transplantation, the indicated doses of mitochondria were given along with the bone marrow. (A) survival curve (B) illness severity including weight loss, and GVHD scores. (*$p < 0.05$, **$p < 0.01$, ***$p < 0.001$, ****$p < 0.0001$; n- number of animals).

6) **TBI conditioning increases circulating cell free mitochondria in patients undergoing HSCT and correlates with the incidence of GVHD.**

Serial samples collected from HSCT patients prior to initiation of conditioning regimen (pre-conditioning), day of transplant (day 0), days 7 (+7) and 14 (+14) following HSCT was evaluated for abundance of extracellular mitochondria in circulation. (A) MTG positive events represented as fold induction relative to the MTG positive events in the pre-conditioning sample of each patient (B). Comparison of mitochondrial levels in samples collected at the indicated times between patients with and without GVHD post HSCT. (*$p < 0.05$)

Table Legend:

1. Demographics for the cohort of patients who received HSCT; including primary diagnosis, HLA molecular typing, transplant conditioning regimen and GVHD prophylaxis.

FIG. 1

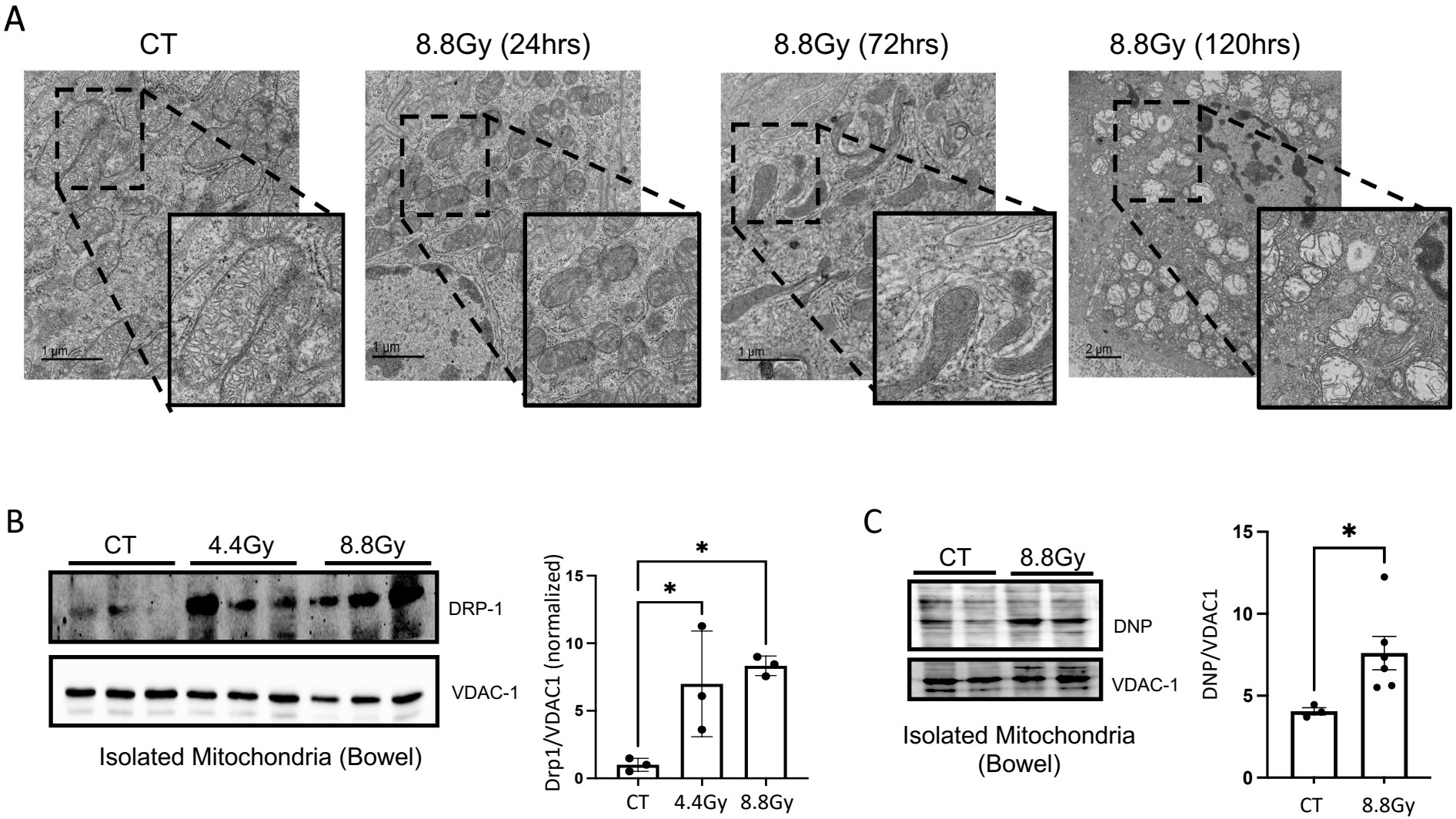
A
CT
8.8Gy (24hrs)
8.8Gy (72hrs)
8.8Gy (120hrs)
1 µm
1 µm
1 µm
2 µm
B
CT
4.4Gy
8.8Gy
DRP-1
VDAC-1
Isolated Mitochondria (Bowel)
Drp1/VDAC1 (normalized)
15
10
5
0
*
*
CT
4.4Gy
8.8Gy
C
CT
8.8Gy
DNP
VDAC-1
Isolated Mitochondria (Bowel)
DNP/VDAC1
15
10
5
0
*
CT
8.8Gy

FIG. 2

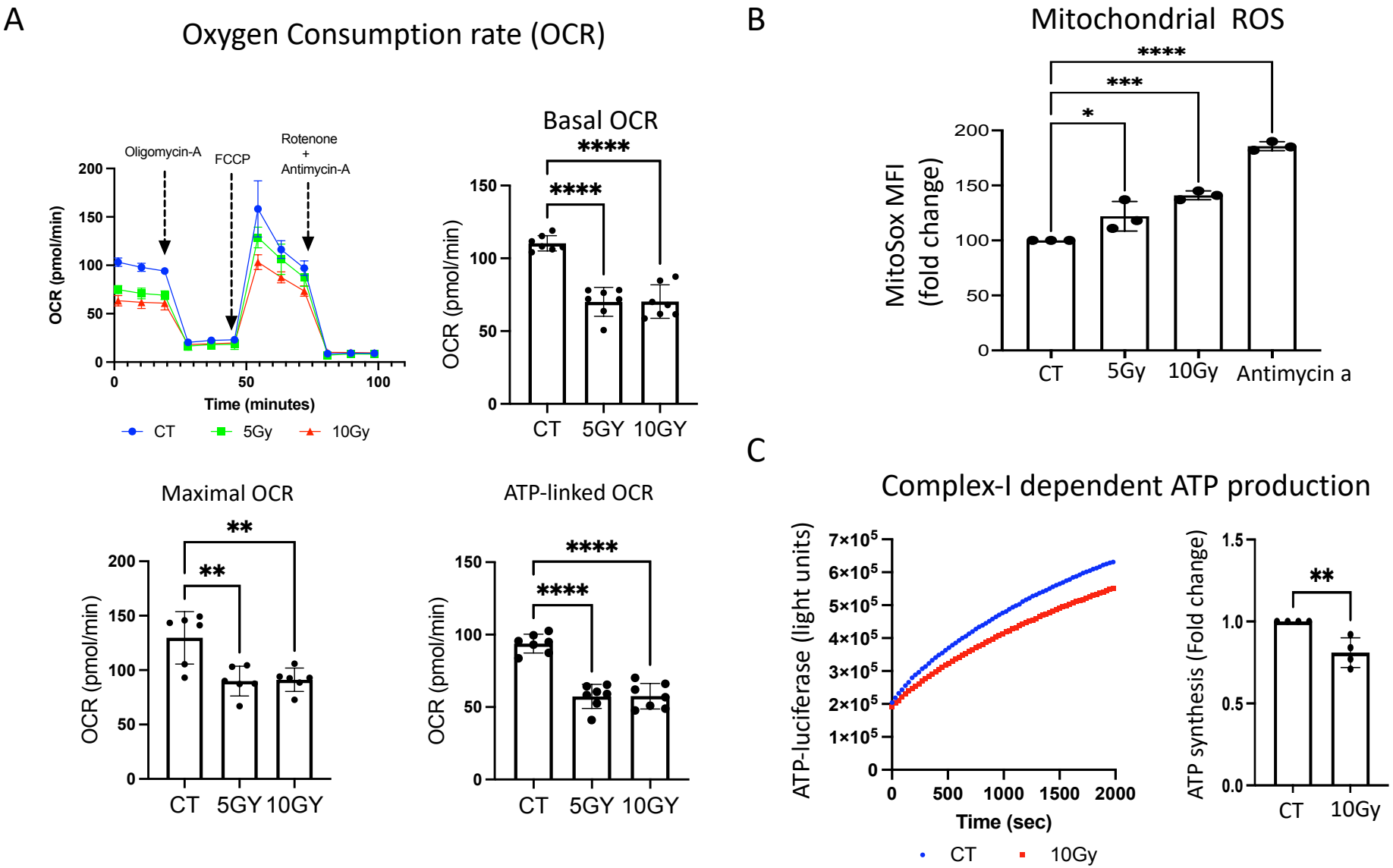
A
Oxygen Consumption rate (OCR)
Oligomycin-A
FCCP
Rotenone + Antimycin-A
OCR (pmol/min)
Time (minutes)
CT
5Gy
10Gy
Basal OCR
****
****
OCR (pmol/min)
CT
5GY
10GY
Maximal OCR
**
**
OCR (pmol/min)
CT
5GY
10GY
ATP-linked OCR
****
****
OCR (pmol/min)
CT
5GY
10GY
B
Mitochondrial ROS
****
***
*
MitoSox MFI (fold change)
CT
5Gy
10Gy
Antimycin a
C
Complex-I dependent ATP production
ATP-luciferase (light units)
Time (sec)
CT
10Gy
ATP synthesis (Fold change)
**
CT
10Gy

FIG. 3

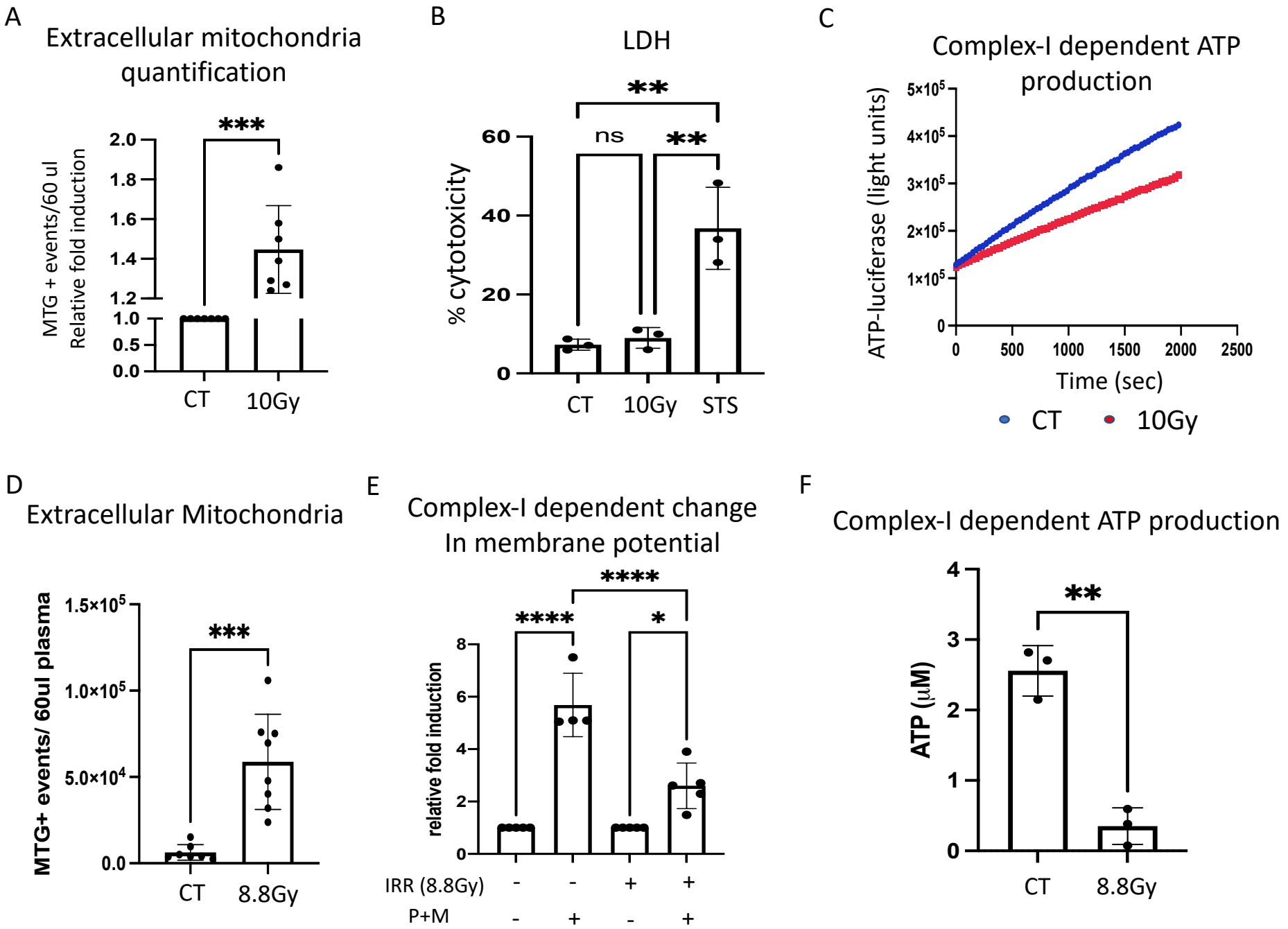
A
Extracellular mitochondria quantification
MTG + events/60 ul
Relative fold induction
2.0
1.8
1.6
1.4
1.2
1.0
0.5
0.0
***
CT
10Gy
B
LDH
% cytotoxicity
60
40
20
0
**
ns
**
CT
10Gy
STS
C
Complex-I dependent ATP production
ATP-luciferase (light units)
5×10^5
4×10^5
3×10^5
2×10^5
1×10^5
0
0
500
1000
1500
2000
2500
Time (sec)
CT
10Gy
D
Extracellular Mitochondria
MTG+ events/ 60ul plasma
1.5×10^5
1.0×10^5
5.0×10^4
0.0
***
CT
8.8Gy
E
Complex-I dependent change In membrane potential
relative fold induction
8
6
4
2
0
****
****
*
IRR (8.8Gy) - - + +
P+M - + - +
F
Complex-I dependent ATP production
ATP (μM)
4
3
2
1
0
**
CT
8.8Gy

FIG. 4

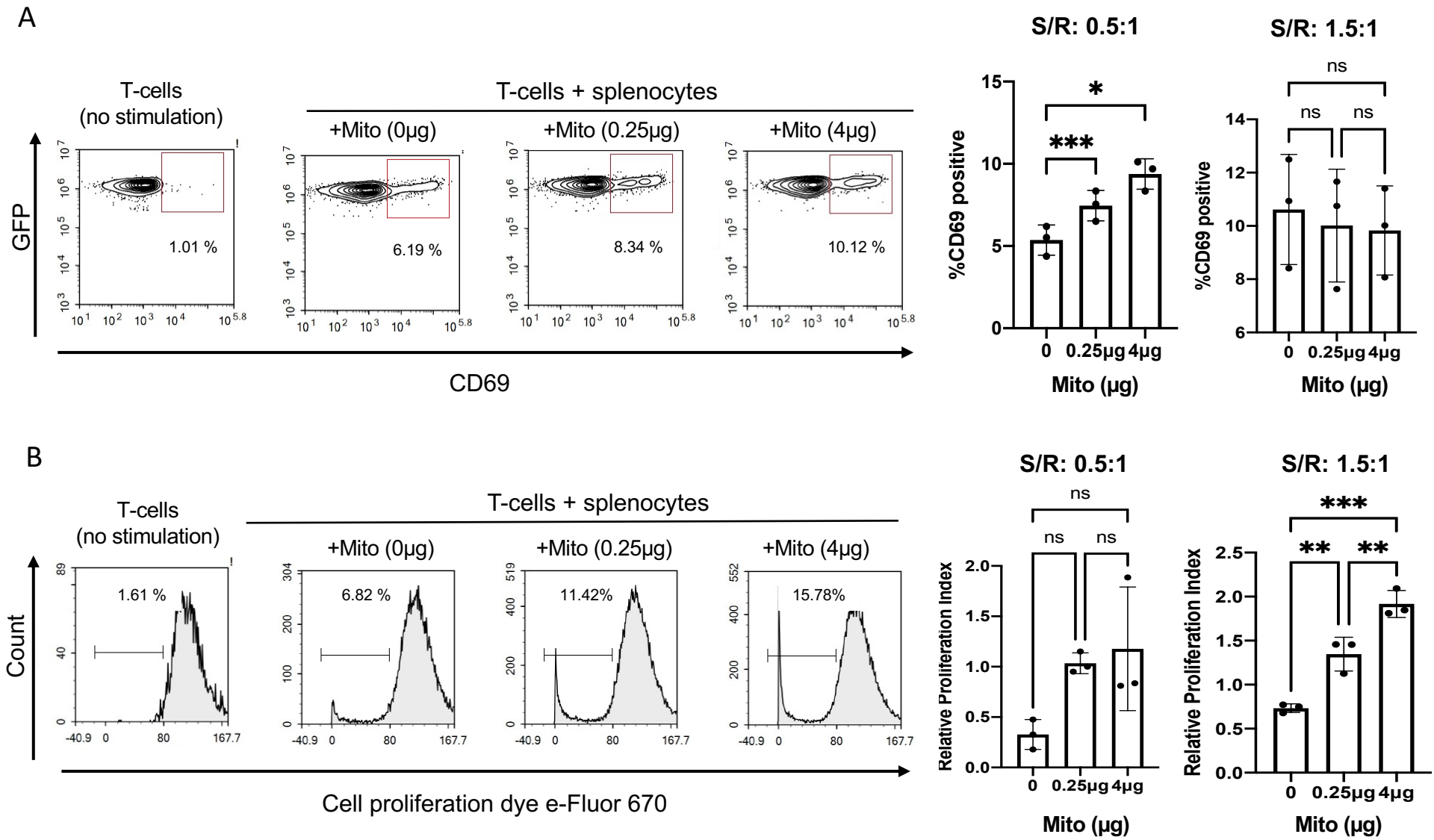
A
T-cells
(no stimulation)
T-cells + splenocytes
+Mito (0μg)
+Mito (0.25μg)
+Mito (4μg)
GFP
1.01 %
6.19 %
8.34 %
10.12 %
CD69
S/R: 0.5:1
S/R: 1.5:1
%CD69 positive
Mito (μg)
0
0.25μg
4μg
*
***
ns
B
Count
1.61 %
6.82 %
11.42%
15.78%
Cell proliferation dye e-Fluor 670
Relative Proliferation Index
**

FIG. 5

A

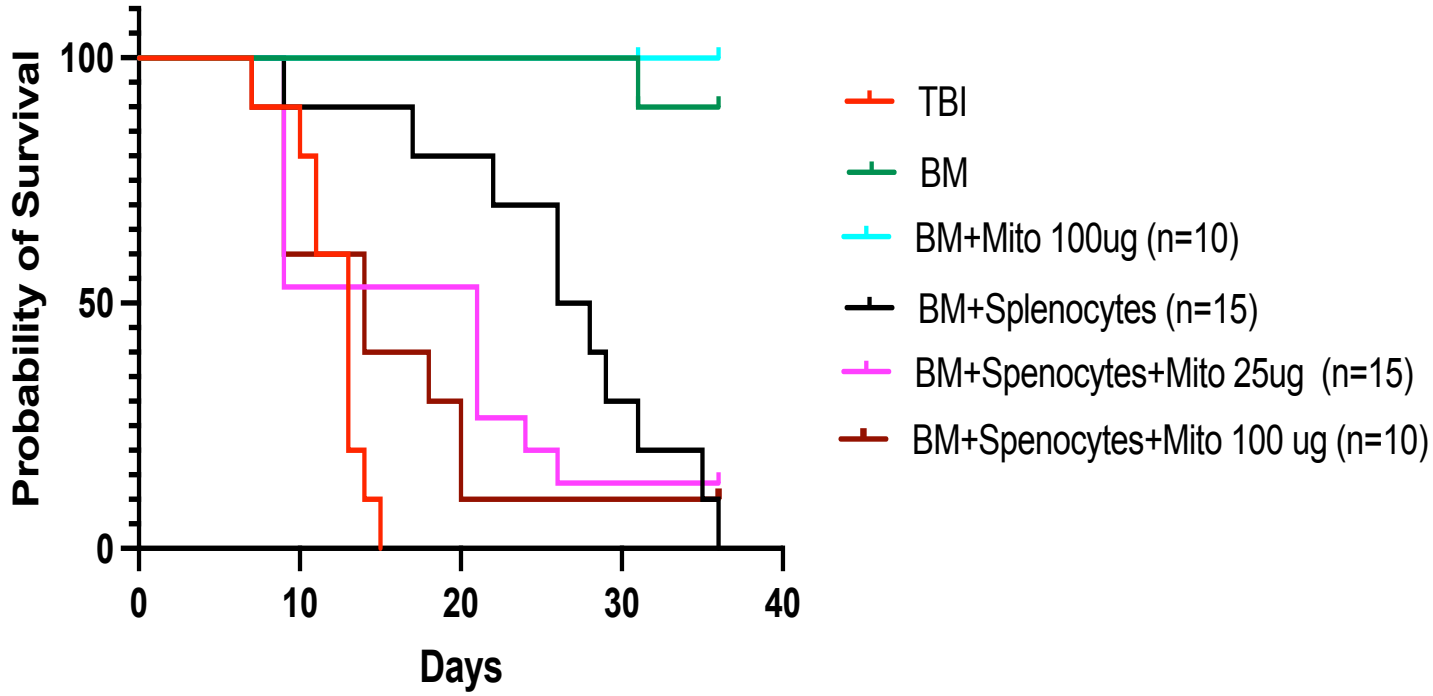

B

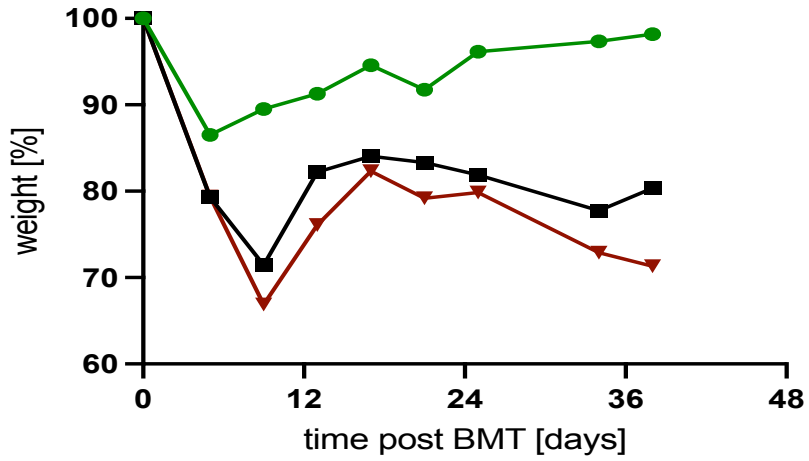

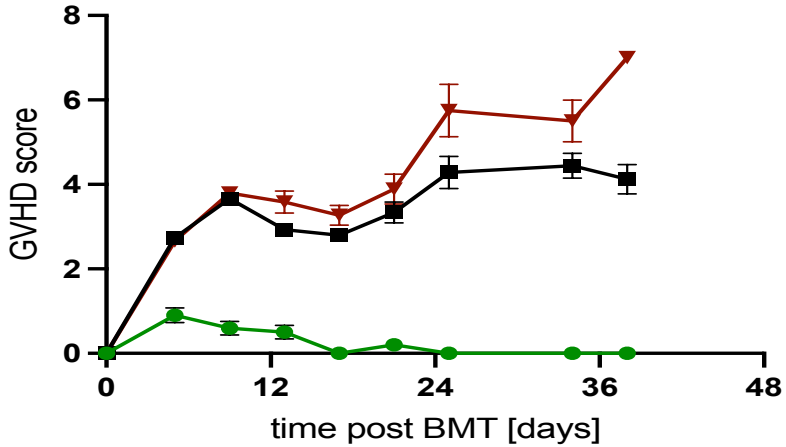

TBI + BM

TBI + BM + Splenocytes

TBI + BM + Splenocytes + Mito (100ug)

FIG. 6

A

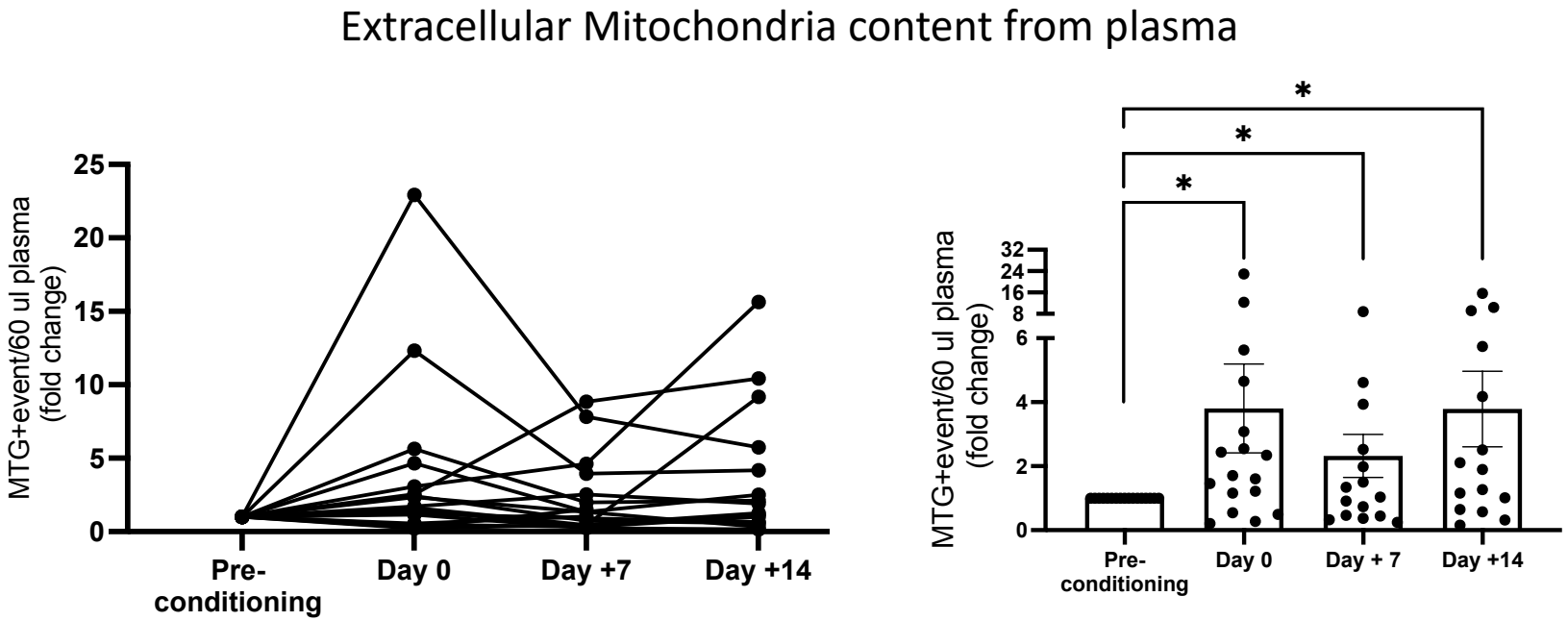
Extracellular Mitochondria content from plasma
MTG+event/60 ul plasma (fold change)
25
20
15
10
5
0
Pre-conditioning
Day 0
Day +7
Day +14
*
*
*
32
24
16
8
6
4
2
0
Pre-conditioning
Day 0
Day + 7
Day +14

B

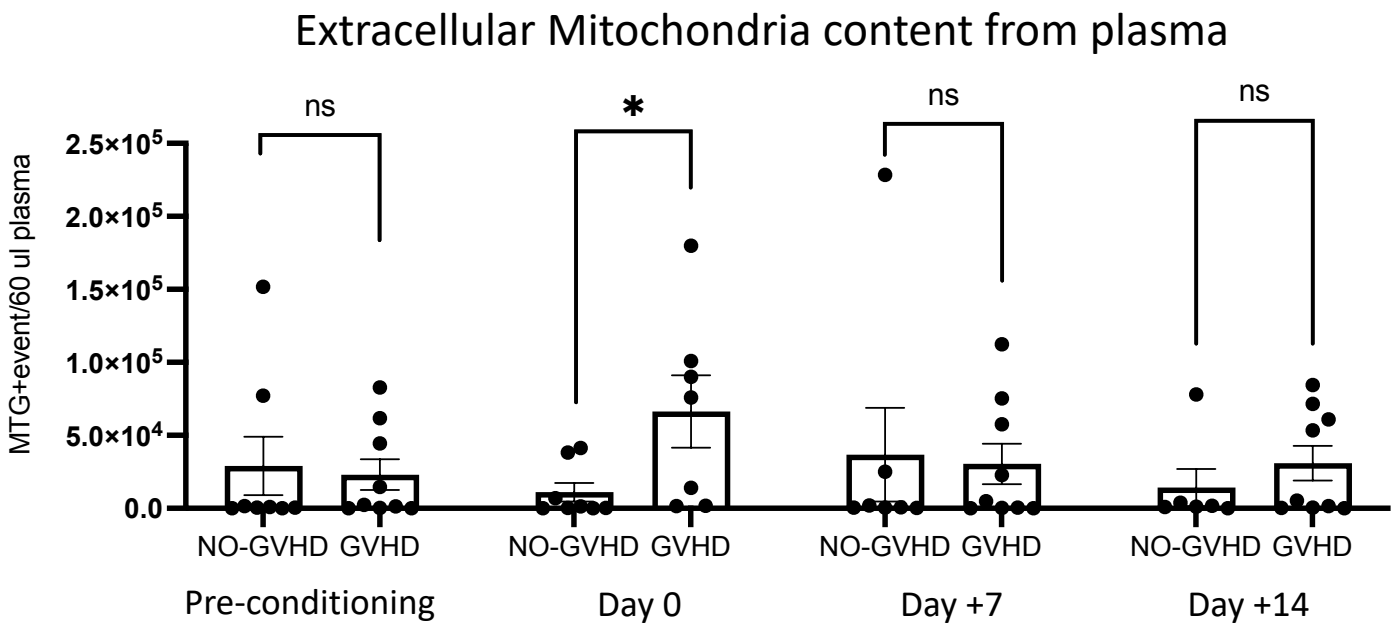
Extracellular Mitochondria content from plasma
MTG+event/60 ul plasma
2.5×10^5
2.0×10^5
1.5×10^5
1.0×10^5
5.0×10^4
0.0
ns
*
ns
ns
NO-GVHD GVHD
NO-GVHD GVHD
NO-GVHD GVHD
NO-GVHD GVHD
Pre-conditioning
Day 0
Day +7
Day +14